

ECG Morphological Variability in Beat Space for Risk Stratification After Acute Coronary Syndrome

Yun Liu, BS; Zeeshan Syed, PhD; Benjamin M. Scirica, MD, MPH; David A. Morrow, MD, MPH; John V. Guttag, PhD; Collin M. Stultz, MD, PhD

Background—Identification of patients who are at high risk of adverse cardiovascular events after an acute coronary syndrome (ACS) remains a major challenge in clinical cardiology. We hypothesized that quantifying variability in electrocardiogram (ECG) morphology may improve risk stratification post-ACS.

Methods and Results—We developed a new metric to quantify beat-to-beat morphologic changes in the ECG: morphologic variability in beat space (MVB), and compared our metric to published ECG metrics (heart rate variability [HRV], deceleration capacity [DC], T-wave alternans, heart rate turbulence, and severe autonomic failure). We tested the ability of these metrics to identify patients at high risk of cardiovascular death (CVD) using 1082 patients (1-year CVD rate, 4.5%) from the MERLIN-TIMI 36 (Metabolic Efficiency with Ranolazine for Less Ischemia in Non-ST-Elevation Acute Coronary Syndrome—Thrombolysis in Myocardial Infarction 36) clinical trial. DC, HRV/low frequency–high frequency, and MVB were all associated with CVD (hazard ratios [HRS] from 2.1 to 2.3 [$P<0.05$ for all] after adjusting for the TIMI risk score [TRS], left ventricular ejection fraction [LVEF], and B-type natriuretic peptide [BNP]). In a cohort with low-to-moderate TRS (N=864; 1-year CVD rate, 2.7%), only MVB was significantly associated with CVD (HR, 3.0; $P=0.01$, after adjusting for LVEF and BNP).

Conclusions—ECG morphological variability in beat space contains prognostic information complementary to the clinical variables, LVEF and BNP, in patients with low-to-moderate TRS. ECG metrics could help to risk stratify patients who might not otherwise be considered at high risk of CVD post-ACS. (*J Am Heart Assoc.* 2014;3:e000981 doi: 10.1161/JAHA.114.000981)

Key Words: morphological variability • risk stratification acute coronary syndrome

Risk stratification after acute coronary syndrome (ACS) involves integrating a diverse array of clinical information. Risk scores, such as Global Registry of Acute Coronary Events (GRACE) and Thrombolysis In Myocardial Infarction (TIMI), aid in this process by incorporating clinical information, such as cardiac risk factors and biomarker data.^{1,2} Unfortunately, existing metrics such as these only identify a subset

From the Institute for Medical Engineering and Sciences, Massachusetts Institute of Technology and Harvard-MIT Division of Health Sciences and Technology, Cambridge, MA (Y.L., C.M.S.); Electrical and Computer Engineering, University of Michigan, Ann Arbor, MI (Z.S.); TIMI Study Group, Cardiovascular Division, Department of Medicine, Brigham and Women's Hospital, and Harvard Medical School, Boston, MA (B.M.S., D.A.M.); MIT Department of Electrical Engineering and Computer Science, Cambridge, MA (J.V.G., C.M.S.).

Accompanying Figures S1 through S2 and Tables S1 through S12 are available at <http://jaha.ahajournals.org/content/3/3/e000981/suppl/DC1>

Correspondence to: Collin M. Stultz, MD, PhD, Room 36-796, 77 Massachusetts Avenue, Cambridge, MA 02139. E-mail: cmstultz@mit.edu

Received April 16, 2014; accepted May 29, 2014.

© 2014 The Authors. Published on behalf of the American Heart Association, Inc., by Wiley Blackwell. This is an open access article under the terms of the Creative Commons Attribution-NonCommercial License, which permits use, distribution and reproduction in any medium, provided the original work is properly cited and is not used for commercial purposes.

of high-risk patients. For example, the top 2 deciles of the GRACE score and a high TIMI risk score captured 67% and 40% of the deaths, respectively.^{1,2} That a significant number of deaths will occur in populations that are not traditionally considered to be high risk highlights a need for tools to discriminate risk further.³ In this regard, the use of computational biomarkers may provide additional information that could improve our ability to identify high-risk patient subgroups.⁴ Indeed, several studies showed that electrocardiogram (ECG)-derived computational metrics significantly improve the ability to risk stratify in subgroups with relatively preserved left ventricular ejection fraction (LVEF).^{4–7}

ECG-based metrics can be broadly divided into ones that analyze heart rate changes and ones that analyze changes in morphology. There are data to suggest that heart-rate–based metrics, such as heart rate variability (HRV),^{8,9} deceleration capacity (DC),⁵ heart rate turbulence (HRT),^{6,10} severe autonomic failure (SAF),⁷ and heart rate motifs,¹¹ measure autonomic modulation of heart rate. Morphology-based metrics include T-wave alternans (TWA),¹² which is designed to measure specific alternating changes in cardiac repolarization, morphologic variability (MV),¹³ which is designed to quantify the beat-to-beat morphologic variability in ECG

signals, and symbolic mismatch,¹⁴ which is designed to uncover anomalous patterns of beats.

In this study, we present a new method of quantifying ECG morphologic variability for risk stratification after non-ST-segment elevation (NSTE)-ACS and compare our metric with published metrics. This is the first study to explore the utility of ECG metrics for further risk stratification among patients that are not currently considered to be high risk, as assessed by the TIMI risk score (TRS), LVEF, and B-type natriuretic peptide (BNP).¹⁵

Methods

Population

Two patient populations were used in this work, a derivation¹⁶ and a validation cohort,¹⁷ from 2 clinical trials of patients with NSTE-ACS. The derivation cohort consisted of 765 patients, with 14 deaths within 90 days. The derivation cohort was used to derive parameters for a new MV risk metric (morphologic variability in beat-space [MVB], described below) and was the same population that the original MV metric was derived from.¹³

We then tested the ability of each ECG-based metric to identify high-risk patients on the validation cohort, consisting of the placebo arm of the MERLIN-TIMI 36 (Metabolic Efficiency with Ranolazine for Less Ischemia in Non-ST-Elevation Acute Coronary Syndrome—Thrombolysis in Myocardial Infarction 36¹⁸) clinical trial, which had a median follow-up of 1 year. The treatment arm was not included because previous studies suggested that ranolazine could have antiarrhythmic properties,¹⁹ thus potentially affecting the ECG. In order to compare our proposed metric with established clinical measures, we only included patients that had measured values for both the LVEF and BNP (N=1082; 1-year cardiovascular death [CVD] rate, 4.5%). In addition, we evaluated the performance of these metrics on “low-risk” patients identified based on information that is available shortly after presentation, the TRS, and BNP. The first subpopulation had low-to-moderate TRS (TRS ≤4; N=864; 1-year CVD death rate, 2.7%), whereas the second subpopulation had an even lower CVD rate (TRS ≤4 and BNP ≤80 pg/mL; N=538; 1-year CVD rate, 1.6%). We also explored the utility of the risk metrics in other low-risk subpopulations based on combinations of TRS, BNP, and LVEF. CVD was adjudicated by a clinical events committee blinded to the ECG results.¹⁸ The protocol was approved by the local or central institutional review board at all participating centers.

MVB

The risk metric, MVB, quantifies beat-to-beat variability in ECG signals and is an evolution of a previously described metric,

MV.¹³ Unlike TWA, which only considers alternating morphologic changes in the ST segment or T wave, MV quantifies morphologic changes in the entire beat, including the TP segment. A key parameter in MV is the diagnostic frequency of 0.30 to 0.55 Hz,¹³ which states that beat-to-beat variability in ECG morphology in this frequency band is prognostic. Taking the inverse of these 2 frequency values gives the temporal periods 3.3 and 1.8 seconds, respectively, implying that high variability roughly every 2 to 3 seconds is prognostic. However, as a result of beat-to-beat variation in heart rate, cardiac activity is periodic with respect to heart beats instead of with respect to time (Figure 1). Accordingly, we speculated that it might be useful to analyze frequency relative to heartbeats, rather than relative to time. This changed the analysis space from time to beats and, consequently, changed the frequency domain (units of Hz) to a “beat frequency” domain (units of cycles/beats). This is equivalent to the interval spectrum²⁰ and beatquency^{21,22} reported in earlier studies. For ease of interpretation, we report the beat-frequency bands as “every x beats.”

The MVB was calculated within both the derivation and validation cohorts using Holter ECG recorded at 128 Hz for each patient. Up to 7 days of ECG records were available in both cohorts (mean, 4.2 days in derivation, 6.2 days in validation), and the first 24 hours were used. Many steps are similar to morphologic variability computation,²³ and the important steps are briefly described here. The ECG was first preprocessed using the Signal Quality Index package as implemented in Physionet^{24,25} to help ensure that only normal

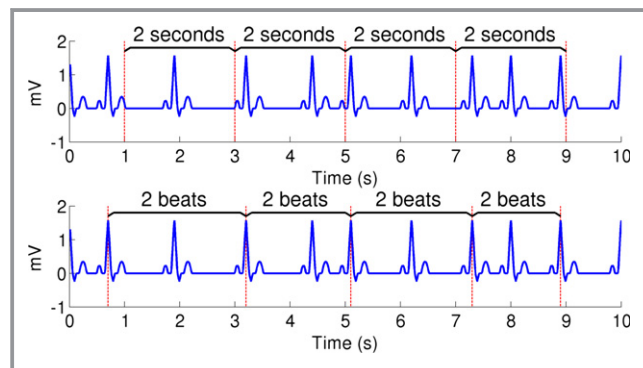


Figure 1. Comparison of periodic events with respect to time (top) and heartbeats (bottom). ECG signals are identical and have average heart rates of 60 bpm. Red lines represent a hypothetical morphological change at a rate of every 2 seconds (0.5 Hz, top) or every 2 beats (0.5 cycles/beat, bottom). If events are periodic in time, each event may be associated with a different part of a beat. However, events that are periodic in beat space are associated with specific cardiac events, the R-wave in this hypothetical example. By performing beat-frequency analysis in MVB (Figure 2), we propose to examine ECG variability of the latter type. MVB indicates morphologic variability in beat space.

beats are studied. Next, baseline wander was removed by subtracting the median filtered signal.²⁶ The ECG signal amplitude was then normalized by dividing each ECG signal by the mean R-wave amplitude for that patient. For example, if the mean R-wave amplitude of the patient is 1.5, the entire ECG signal is divided by 1.5; isoelectric segments are unaffected, and the rest of the signal is scaled appropriately. This step corrects for calibration errors and interpatient differences and enables more-meaningful comparison of morphological differences. Next, the ECG signal was converted into a beat-to-beat variability time series termed the morphologic distance (MD) time series. The MD time series quantified beat-to-beat morphologic changes in the ECG signal; each MD point was defined by the sum of the squared differences between the aligned beats (Figure 2, step 1). Notably, the MD time series in MVB had the heartbeat index (1, 2, 3, and so on) as the x-axis instead of time. Next, the MD time series (in beat space) was segmented into 5-minute intervals, and each 5-minute segment was transformed to the frequency domain, in a manner similar to what is done for HRV.⁸ For each 5-minute interval, the energy in a diagnostic beat frequency was computed (Figure 2, step 2). This diagnostic beat frequency was optimized in the derivation cohort of patients with ACS (described below). The 90th percentile of these energies from all of the 5-minute windows was termed the MVB for that patient (Figure 2, step 3). Figure 2 summarizes the steps in MVB computation, including the optimal diagnostic beat frequency.

The optimal diagnostic beat frequency was searched in the derivation cohort over the range of every 2 beats to every 100 beats (Figure S1). For every possible start and end beat frequency, we computed the 90th percentile of the energy in that beat frequency band over all 5-minute windows in the day. The AUC (area under the receiver operating characteristic curve)²⁷ was then computed for that diagnostic beat frequency across all patients in the derivation cohort with the outcome of death within 90 days of follow-up. Finally, the beat-frequency range with the highest AUC is chosen to be the optimal diagnostic beat frequency. The AUCs are presented as a heat map, where each point in the heat map corresponds to the AUC for MVB computed using a specific beat-frequency range as indicated by the respective axes (Figure S1). We obtained an optimal diagnostic beat frequency of every 2 to 7 beats, with an AUC of 0.725. A similar procedure was previously applied to optimize a diagnostic frequency.¹³

Analysis of MVB in Specific ECG Segments

To analyze the physiology underlying the variability measured by MVB, we quantified MVB resulting from partial segments of the ECG. First, the ECG signal is preprocessed as per the

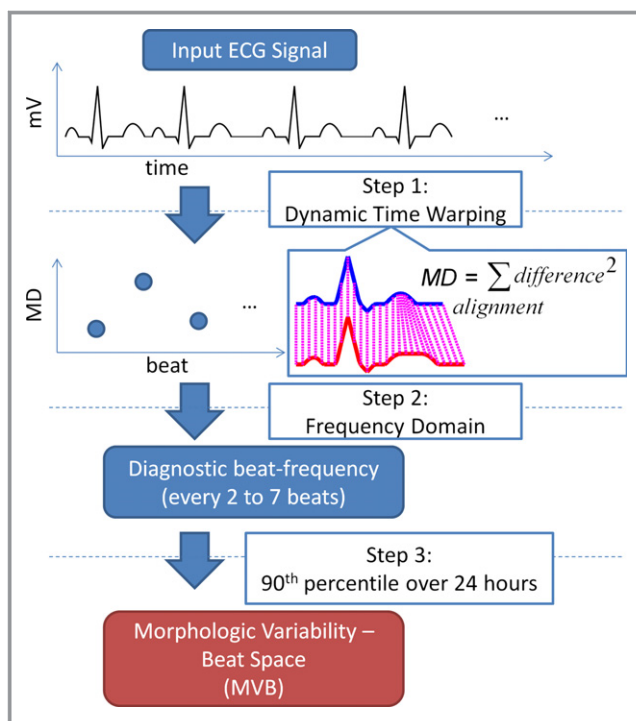


Figure 2. Overview of morphologic variability in beat space (MVB) computation. Step 1: The input ECG signal is first converted into a beat-to-beat distance time series termed the morphologic distance (MD) time series. This conversion is performed by dynamic time warping (DTW), an algorithm that ensures beats are aligned before comparison. DTW compares the blue T wave with the extended red T wave above; a direct subtraction would compare the late blue T wave with the mid red T wave in the above DTW schematic. Each pair of adjacent beats generates a single MD value; N beats generates (N-1) MD values. In MVB computation, the MD time series has the “beat index” instead of “time” for the x-axis. Step 2: The MD time series is segmented into 5-minute windows. Next, for each 5-minute window, the MD time series is converted to the beat-frequency domain and the energy in the diagnostic beat-frequency is summed. Step 3: The 90th percentile of these energies over all 5-minute windows in 24 hours is termed the MVB for that patient.

steps in MVB. Next, the beat-to-beat morphologic distance time series is computed for each quarter of the ECG segment, resulting in 4 values for each original MD value: MD1, MD2, MD3, and MD4; $MD = MD1 + MD2 + MD3 + MD4$. This results in 4 new time series, which summarize the variability in partial segments of the ECG. The remaining steps of conversion to the frequency domain, summing the energy in the range of every 2 to 7 heartbeats, and taking the 90th percentile, are identical.

Comparison With Published Risk Metrics

MVB was compared with other published risk metrics: HRV,⁸ HRT,⁶ DC,⁵ SAF,⁷ TWA (computed using a fully automated version of the modified moving average²⁸), TRS,² LVEF, and BNP.¹⁵ Several HRV metrics were computed: low frequency/

high frequency (LF/HF); standard deviation of average NN intervals (SDANN); heart rate variability triangular index (HRVI); average standard deviation of NN intervals (ASDNN); standard deviation of NN intervals (SDNN); proportion of consecutive NN intervals that differ by more than 50 ms (PNN50); and root mean square of successive differences (RMSSD).⁸ All ECG metrics were computed using previously described methods,⁴ and all metrics were dichotomized for statistical analysis (below).

Statistical Analysis

We evaluated these metrics based on uni- and multivariable 1-year hazard ratios (HRs). HRs were computed using Cox's proportional hazards regression model.²⁹ Continuous risk metrics were dichotomized at the highest (or lowest) quartile, as appropriate, for all continuous metrics (MVB, HRV, DC, and TWA). This enabled meaningful comparisons of HRs for 2 reasons: (1) none of the established cutoffs were derived for the specific populations analyzed here, and (2) this ensured equal proportions of patients in each metric's high-risk category. LVEF and BNP were dichotomized at $\leq 40\%$ and $> 80 \text{ pg/mL}$,¹⁵ respectively. For categorical metrics with more than 2 categories (TRS and HRT), the highest-risk categories were used: TRS ≥ 5 and HRT = 2. The HRs relative to other published thresholds (DC ≤ 2.5 , DC ≤ 4.5 , HRT ≥ 1 , DC ≤ 2.5 versus > 4.5 , HRT = 2 versus 0) are reported in the Supporting Information. After dichotomization, each metric was replaced by a binary value; for example, TRS is "1" if TRS ≥ 5 , and "0" otherwise. Each multivariable HR was computed by including TRS, LVEF, BNP, and a single ECG metric.

We also constructed multivariable models, including TRS, LVEF, and BNP, and assessed the AUC of these models relative to models that also included MVB. Because meaningful improvements in discrimination can be masked by small changes in AUC,³⁰ the statistical difference in the model was quantified by the category-free net reclassification index (cfNRI).³¹ Models were adjusted, as appropriate, in lower-risk subpopulations (Table S10).

Results

Association Between Risk Metrics and CVD in the Validation Cohort

Baseline characteristics of the validation cohort and low-risk subpopulations are shown in Table 1. In a univariable analysis, TRS, HRV, BNP, DC, LVEF, MVB, and HRT were all associated with the risk of CVD (Table 2). After adjusting for TRS, BNP, and LVEF, only DC, HRV-LF/HF, and MVB remained significantly associated with CVD (HRs from 2.1 to 2.3; $P < 0.05$ for all [Table 2]).

The cfNRI of the addition of MVB to models including TRS, LVEF, and BNP are presented in Table S10. The nonevent cfNRI was 52% (95% confidence interval [CI], 45 to 57). The cfNRI was 45% (95% CI, 13 to 76). The AUC of the model improved from 0.735 to 0.761 after inclusion of MVB (Table S10), and the model was well calibrated (Table S11).

Association Between Risk Metrics and CVD in Lower-Risk Subpopulations

A total of 22 (49%) of 45 CVD occurred in the subgroup with TRS ≤ 4 (N=864), and this subgroup had a 1-year CVD rate of 2.7%. In this population, MVB, HRV-LF/HF, BNP, and DC were significantly associated with CVD (Table 3). After adjusting for LVEF and BNP, only MVB remained significantly associated with CVD (HR, 3.0; $P = 0.014$ [Table 3]). Figure 3A shows the Kaplan-Meier curves for MVB in this population.

In a subgroup of patients with even lower CVD rate (TRS ≤ 4 and BNP $\leq 80 \text{ pg/mL}$; N=538; 1.6% 1-year CVD, rate), MVB was significantly associated with CVD (HR, 8.9; $P = 0.007$ [Table 4]). After adjusting for LVEF, MVB remained significantly associated with CVD (adjusted HR, 7.8, respectively; $P = 0.014$ [Table 4]). Figure 3B shows the Kaplan-Meier curves for MVB in this population. Similar results were found in other low-risk subpopulations based on a combination of TRS and LVEF and/or BNP: MVB, but not the other ECG metrics, was significantly associated with CVD (Tables 5 and S3 through S6).

The cfNRI of MVB in the lower-risk subpopulations are presented in Table S10. Reference models included LVEF and/or BNP, as appropriate. The nonevent cfNRI were nearly identical in all subpopulations ($\approx 52\%$; 95% CI, 44 to 58), whereas the cfNRI ranged from 60% to 100%, with a larger (but still significant) CI resulting from the small numbers of CVD. The AUC of the models improved from 0.661 or less to at least 0.725 after inclusion of MVB (Table S10), and the models were well calibrated (Table S11).

Choosing an Optimal Threshold for MVB

The results presented above use the upper quartile value as the high-risk threshold. This facilitates comparison of the various ECG metrics. However, such a choice is not useful clinically because it is difficult to know *a priori* what the upper quartile would be for any given set of patients. In this regard, a set cut-off value would be the most useful. We therefore used a set cut-off value (2.9), corresponding to the upper-quartile value in our derivation cohort, to calculate HRs in our validation cohorts. The results argue that a fixed cutoff of 2.9 yields HRs that are similar to what was achieved with using cohort-specific upper quartiles (Tables S2 through S6, see row MVB > 2.9). We have also presented the rates of CVDs as a

Table 1. Baseline Patient Characteristics for Validation Cohort and Lower-Risk Subpopulations

	Validation Cohort (EF and BNP)	TRS ≤4	TRS <4 and BNP ≤80
N	1082	864	538
Cardiovascular deaths (CVD)	45 (4.5%)	22 (2.7%)*	8 (1.6%)*
Age, years, median (IQR)	63 (55 to 71)	61 (54 to 69)*	58 (53 to 66)*
Female, %	37	37	36
BMI, median (IQR)	28 (25 to 32)	29 (26 to 32)	29 (26 to 33)
Diabetes mellitus, %	35	32	34
Hypertension, %	78	75	76
Current smoker, %	24	26	26
Previous MI, %	36	28*	27*
Index event, %			
Unstable angina	52	52	64*
MI	48	48	36*
ST depression ≥1 mV, %	39	35*	27*
TIMI risk score, %			
Low (1 to 2)	25	31*	35*
Moderate (3 to 4)	55	69*	65*
High (5 to 7)	20	0*	0*
LVEF measured, %	100	100	100
LVEF ≤40% (%)	12	10	7*
BNP measured, %	100	100	100
BNP >80 pg/mL (%)	42	38	0*

*Statistical significant difference (at the 5% level), compared to the validation cohort. BMI indicates body mass index; BNP, B-type natriuretic peptide; EF, ejection fraction; LVEF, left ventricular ejection fraction; TIMI, Thrombolysis In Myocardial Infarction; TRS, TIMI risk score.

function of MVB quartiles in the validation cohort and low-risk subpopulations (Figure S2).

Correlation of MVB With Other Variables

We also measured the correlation of MVB with the other ECG metrics (Table S8). The correlation coefficients were below 0.5 for all metrics. In particular, MVB was uncorrelated with TWA, the other morphology-based ECG metric analyzed in this study ($r=0.044$). The correlation of MVB with other baseline characteristics are presented in Table S9. The correlation coefficient was 0.361 for heart rate and below 0.15 for all other baseline characteristics.

Analysis of MVB in Specific ECG Segments

To investigate the physiology underlying the variability measured by MVB, we computed MVB using partial segments of the ECG (see Methods). In the derivation cohort, the 4 quarters result in AUCs of 0.608, 0.629, 0.644, and 0.687,

respectively, lower than that for MVB computed using the entire ECG (0.725) (Table S12).

Discussion

In the present study, we evaluated the ability of several ECG-based risk metrics to risk stratify patients in conjunction with well-established clinical risk tools, such as the TRS, LVEF, and BNP. Existing risk metrics typically only identify a subset of the high-risk patients. For example, patients with a high TRS were at the highest relative risk of CVD (HR, 4.42), but only accounted for half of all CVD. Therefore, a low-to-moderate risk population still contains a significant number of adverse events, and the lack of appropriate risk stratification in such populations remains a clinical deficiency. We find that in a population with a low-to-moderate TRS, MVB was the only ECG metric that was significantly associated with CVD after adjusting for LVEF and BNP (Table 3). This relationship was similar in other low-risk subpopulations (Tables 4 and 5).

Table 2. Association of ECG-Based Risk Metrics With CVD After Adjusting for LVEF, BNP, and TRS on the Validation Cohort (1-year CVD rate, 4.5%)

Risk Metric	Univariable 1-Year Hazard Ratio (95% Confidence Intervals [CI])	P Value	Multivariable 1-Year Hazard Ratio (Adjusted for LVEF, BNP, and TRS) (95% CI)	P Value
TRS	4.42 (2.46, 7.92)	0.000	—	—
BNP	3.20 (1.70, 6.02)	0.000	—	—
LVEF	2.76 (1.43, 5.34)	0.003	—	—
DC*	3.01 (1.68, 5.41)	0.000	2.26 (1.22, 4.17)	0.009
HRV-LF/HF*	3.25 (1.81, 5.83)	0.000	2.21 (1.20, 4.09)	0.011
MVB*	2.70 (1.50, 4.85)	0.001	2.11 (1.15, 3.89)	0.016
HRV-SDANN	1.84 (1.01, 3.36)	0.048	1.53 (0.83, 2.81)	0.171
HRV-HRVI	1.37 (0.73, 2.57)	0.334	1.12 (0.59, 2.13)	0.728
HRV-ASDNN	1.36 (0.72, 2.55)	0.344	1.09 (0.58, 2.07)	0.790
HRV-SDNN	1.21 (0.64, 2.31)	0.558	1.03 (0.54, 1.98)	0.925
TWA	1.11 (0.57, 2.15)	0.758	0.82 (0.39, 1.71)	0.597
HRT2	1.37 (0.58, 3.25)	0.474	0.77 (0.32, 1.89)	0.574
HRV-PNN50	0.75 (0.36, 1.55)	0.432	0.76 (0.37, 1.58)	0.459
HRV-RMSSD	0.64 (0.30, 1.38)	0.255	0.75 (0.35, 1.61)	0.452
SAF	1.18 (0.42, 3.31)	0.750	0.68 (0.24, 1.97)	0.481

Hazard ratios are computed relative to the upper quartile value in this population, unless otherwise indicated; hazard ratios computed relative to other thresholds are shown in Table S2. ASDNN indicates average standard deviation of NN intervals; BNP, B-type natriuretic peptide; DC, deceleration capacity; HRT, heart rate turbulence; HRV, heart rate variability; HRVI, heart rate variability triangular index; LF/HF, low frequency/high frequency; LVEF, left ventricular ejection fraction; PNN50, proportion of consecutive NN intervals that differ by more than 50 ms; RMSSD, root mean square of successive differences; SAF, severe autonomic failure; SDANN, standard deviation of average NN intervals; SDNN, standard deviation of NN intervals; TRS, TIMI risk score; TWA, T-wave alternans.

*Metrics with significant multivariable hazard ratios.

Table 3. Association of ECG-Based Metrics With CVD After Adjusting for LVEF and BNP on a Low-to-Moderate Cohort Consisting of all Patients With TRS ≤ 4 (1-Year CVD Rate, 2.7%)

Risk Metric	Univariable 1-Year Hazard Ratio (95% CI)	P Value	Multivariable 1-Year Hazard Ratio (Adjusted for LVEF and BNP) (95% CI)	P Value
BNP	2.93 (1.23, 6.98)	0.015	—	—
LVEF	2.66 (0.98, 7.22)	0.054	—	—
MVB*	3.66 (1.58, 8.48)	0.002	2.99 (1.25, 7.15)	0.014
HRV-LF/HF	3.01 (1.31, 6.95)	0.010	2.32 (0.98, 5.53)	0.057
DC	2.55 (1.10, 5.91)	0.029	1.97 (0.82, 4.73)	0.132
HRT2	2.56 (0.86, 7.67)	0.092	1.85 (0.60, 5.74)	0.284
SAF	2.34 (0.69, 7.99)	0.174	1.59 (0.45, 5.65)	0.474
HRV-SDANN	1.69 (0.71, 4.03)	0.235	1.43 (0.59, 3.45)	0.423
HRV-SDNN	1.69 (0.71, 4.02)	0.239	1.41 (0.59, 3.40)	0.442
HRV-ASDNN	1.38 (0.56, 3.39)	0.478	1.18 (0.48, 2.91)	0.726
HRV-PNN50	0.88 (0.32, 2.38)	0.798	0.93 (0.34, 2.53)	0.890
HRV-HRVI	0.87 (0.32, 2.35)	0.779	0.72 (0.26, 1.98)	0.526
HRV-RMSSD	0.66 (0.22, 1.95)	0.451	0.68 (0.23, 2.00)	0.480
TWA	1.16 (0.45, 2.95)	0.763	0.63 (0.21, 1.88)	0.411

Hazard ratios are computed relative to the upper quartile value in this population, unless otherwise indicated; hazard ratios computed relative to other thresholds are shown in Table S3. ASDNN indicates average standard deviation of NN intervals; BNP, B-type natriuretic peptide; DC, deceleration capacity; HRT, heart rate turbulence; HRV, heart rate variability; HRVI, heart rate variability triangular index; LF/HF, low frequency/high frequency; LVEF, left ventricular ejection fraction; PNN50, proportion of consecutive NN intervals that differ by more than 50 ms; RMSSD, root mean square of successive differences; SAF, severe autonomic failure; SDANN, standard deviation of average NN intervals; SDNN, standard deviation of NN intervals; TRS, TIMI risk score; TWA, T-wave alternans.

*Metrics with significant multivariable hazard ratios.

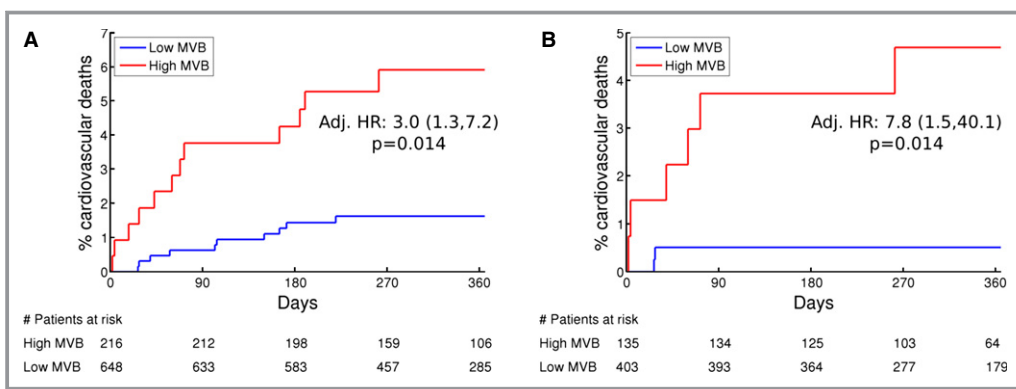


Figure 3. Kaplan-Meier curves demonstrating risk stratification of 2 relatively lower-risk subpopulations using the upper-quartile value in each population (A: TRS ≤ 4 ; B: TRS ≤ 4 and BNP ≤ 80 pg/mL). Numbers of patients remaining in the study at each labeled time point are indicated below the respective labels. BNP indicates B-type natriuretic peptide; MVB, morphologic variability in beat space; TRS, TIMI risk score.

Our data highlight the utility of using a morphology-based ECG metric for risk stratification in populations that are not normally considered to be high risk. It is important to keep in mind, however, that ECG metrics that analyze changes in the heart rate alone have been shown to have utility in other patient populations. Patients with low HRV are associated with increased mortality after myocardial infarction (MI) in multiple studies; for example, in the largest study ($N=1284$), a low HRV-SDNN increased mortality 3-fold during 21 months of follow-up.³² A meta-analysis found that patients with a low HRV-SDNN have a mortality rate that is almost 4 times within

3 years after an MI.³³ In addition, HRT has been shown to identify patients at increased risk of death post-MI^{6,10} and in elderly adults.³⁴ In the prospective study of post-MI patients ($N=1455$), HRT categories 1 and 2 had significant HRs in both the post-MI population and a subgroup with LVEF $>30\%$.⁶ SAF predicted all-cause mortality, CVD, and sudden cardiac death in post-MI patients and a subgroup with LVEF $>30\%$,⁷ and DC was shown to accurately predict death post-MI, especially in patients with LVEF $>30\%.$ ⁵

The other morphology-based metric evaluated in this study, TWA, can be measured in 2 ways³⁵: (1) using specialized

Table 4. Association of ECG-Based Metrics With CVD After Adjusting for LVEF on a Lower-Risk Subpopulation (TRS ≤ 4 and BNP ≤ 80 ; CVD Rate, 1.6%)

Risk Metric	Univariable 1-Year Hazard Ratio (95% CI)	P Value	Multivariable 1-Year Hazard Ratio (Adjusted for LVEF) (95% CI)	P Value
LVEF ≤ 40	4.70 (0.95, 23.29)	0.058	—	—
MVB*	8.91 (1.80, 44.15)	0.007	7.81 (1.52, 40.09)	0.014
HRT2	2.59 (0.31, 21.49)	0.379	2.94 (0.35, 24.72)	0.320
DC	2.99 (0.75, 11.97)	0.121	2.39 (0.55, 10.30)	0.243
HRV-LF/HF	1.76 (0.42, 7.35)	0.441	1.67 (0.40, 7.01)	0.484
HRV-PNN50	0.99 (0.20, 4.90)	0.989	1.02 (0.20, 5.03)	0.985
TWA	1.84 (0.44, 7.70)	0.404	0.98 (0.20, 4.88)	0.984
HRV-ASDNN	0.98 (0.20, 4.86)	0.981	0.90 (0.18, 4.47)	0.893
HRV-RMSSD	0.42 (0.05, 3.41)	0.416	0.39 (0.05, 3.21)	0.383
HRV-SDANN	0.42 (0.05, 3.41)	0.416	0.38 (0.05, 3.09)	0.364
HRV-SDNN	0.42 (0.05, 3.43)	0.420	0.37 (0.04, 3.03)	0.354
SAF	0.00 (0.00, Inf)	0.996	0.00 (0.00, Inf)	0.995
HRV-HRVI	0.00 (0.00, Inf)	0.994	0.00 (0.00, Inf)	0.994

Hazard ratios are computed relative to the upper quartile value in this population, unless otherwise indicated; hazard ratios computed relative to other thresholds are shown in Table S5. ASDNN indicates average standard deviation of NN intervals; DC, deceleration capacity; HRT, heart rate turbulence; HRV, heart rate variability; HRVI, heart rate variability triangular index; LF/HF, low frequency/high frequency; LVEF, left ventricular ejection fraction; PNN50, proportion of consecutive NN intervals that differ by more than 50 ms; RMSSD, root mean square of successive differences; SAF, severe autonomic failure; SDANN, standard deviation of average NN intervals; SDNN, standard deviation of NN intervals; TRS, TIMI risk score; TWA, T-wave alternans.

*Metrics with a significant multivariable hazard ratio.

Table 5. Association of MVB With Cardiovascular Death (CVD) in the Entire Placebo Group and Low-Risk Subpopulations

Population	No. of Patients (CVD Rate)	Hazard Ratio (HR) Adjusted for	HR for MVB (CI), P Value
Entire placebo	1082 (4.5%)	TRS, LVEF, BNP	2.1 (1.2, 3.9), 0.016
TRS ≤4*	864 (2.7%)	LVEF, BNP	3.0 (1.3, 7.2), 0.014
TRS ≤4, LVEF >40*	776 (2.3%)	BNP	3.8 (1.5, 10.2), 0.007
TRS ≤4, BNP ≤80*	538 (1.6%)	LVEF	7.8 (1.5, 40.1), 0.014
TRS ≤4, LVEF >40, BNP ≤80*	503 (1.3%)	—	14.9 (1.7, 127.7), 0.014

Baseline patient characteristics are presented in Table S1. BNP, B-type natriuretic peptide; LVEF, left ventricular ejection fraction; TRS, TIMI risk score.

*Populations and hazard ratios in which the other ECG metrics were not significantly associated with CVD at the 5% level (details in Tables S2 through S6).

equipment to assess microvolt changes in T-wave morphology and (2) using standard Holter monitor data with a modified moving average method (MMA; assessed in this study). Both methods have been evaluated with respect to their ability to predict ventricular arrhythmia, mortality, and sudden cardiac death (SCD) in various patient populations, such as patients with dilated cardiomyopathy, congestive heart failure, and patients who are post-MI.³⁵ In 1 study (N=219), where 91% of the patients had LVEF≥40%, a high TWA (MMA) had a hazard ratio of 17.78 for SCD.³⁶ Thus, all of the existing ECG metrics provide additional information that can be clinically useful in the right patient populations. However, to our knowledge, this is the first study to systematically evaluate the performance of these ECG metrics on patients who would not be identified as high risk on presentation, as defined by their TIMI risk score and their blood BNP concentration.

MVB differs from the aforementioned ECG-based metrics in that it quantifies morphologic differences between “entire” beats, rather than focusing on portions of the ECG signal (such as the ST segment and T wave in TWA). The motivation for deriving a beat-space-based metric (MVB) is the intuition that morphologic changes could be associated with cardiac cycles instead of time (Figure 1). Because high frequencies of abnormal events are cause for greater concern in general, it is not surprising that the repeating frequency of MVB (diagnostic beat frequency) corresponds to high beat frequencies, or equivalently, low values of “every x beats.”

Beat-to-beat morphologic changes in an ECG can arise when unstable islands of ischemia throughout the myocardium present in a probabilistic or random manner.³⁷ Therefore, we postulated that metrics which quantify beat-to-beat morphologic variations may have prognostic power in patients with known CVD; for example, significant beat-to-beat variability may be associated with more ischemic events and poor outcomes, relative to those with less beat-to-beat variability. Moreover, whereas ischemia often manifests during myocardial repolarization, it can also result in morphologic changes elsewhere in the cardiac cycle (eg, in the PR segment and QRS complex).^{38,39} Therefore, we strove

to develop a metric that would quantify the morphologic variability using the entire cardiac cycle. Consistent with this goal, MVB variants that quantify morphologic differences in partial segments of the ECG segment result in poorer discriminative performance.

Among the beat-frequency bands measured by MVB is “every 2 beats.” Although the number 2 is reminiscent of TWA,¹² we find that MVB and TWA are not correlated, suggesting that MVB and TWA measure different aspects of the ECG signal. TWA measures the presence of an ABAB pattern where A and B denote 2 beats having different morphologies—in this case, the morphology difference is isolated to the ST segment and T wave. This ABAB pattern would produce a consistently high MD time series, or “every 1 beat.” As such, this phenomenon would not be measured by our beat-frequency analysis, but would instead correspond mathematically to the mean value of the MD time series.

Limitations

Our study has limitations. First, LVEF and BNP measurements were not available for all patients, reducing the population size relative to the entire placebo arm of the MERLIN-TIMI36 trial. Second, because of the lack of ventricular premature beats for some records, we were unable to compute HRT (and thus SAF) for all patients in the validation cohort. For a data set of this magnitude, it was impractical to perform manual visual inspection of all ECG segments, and therefore we computed TWA in a fully automated implementation of the modified moving average approach. For a similar reason, QT Variability Index (QTVI), which requires manual definition of a template QT interval for each patient,⁴⁰ was not measured. Microvolt ECG records were not recorded for patients in our cohorts, and therefore microvolt TWA was not measured. Thus, the utility of microvolt TWA and QTVI in a population with low-to-moderate TRS remains undetermined. In addition, our ECG signals were recorded at the standard Holter rate of 128 Hz; higher resolutions have been recommended for the evaluation of the HRV metrics,⁸ and the availability of higher-resolution ECG records may improve their performance in

low-risk populations. Because <2% of the patients had documented atrial fibrillation, we were unable to perform a comprehensive analysis of the association of MVB with CVD in this subpopulation. Finally, we did not have all variables required to compute the GRACE¹ risk score. The hypothesis that ECG metrics would be useful in patients with a low-to-moderate GRACE risk score needs to be evaluated in future work.

Conclusions

We have shown that an ECG morphology-based metric may provide incremental risk stratification in patients who would normally be considered to be low-to-moderate risk on presentation as determined by clinical risk scores, levels of BNP, and LVEF. To our knowledge, this is the first study to evaluate the performance of multiple ECG metrics in low-to-moderate risk patients with comprehensive comparison to both BNP and LVEF, and therefore may further improve development of risk-stratification methods (both morphology based and otherwise) specifically for low-risk populations, where a significant number of cardiovascular complications continue to occur.

Sources of Funding

This work was funded by the Agency of Science, Technology and Research (A*STAR), Singapore, Quanta Computer, Taiwan, and General Electric, USA MERLIN-TIMI 36 was supported by CV Therapeutics (now Gilead Sciences).

Disclosures

None.

References

- Granger CB, Goldberg RJ, Dabbous O, Pieper KS, Eagle KA, Cannon CP, Van de Werf F, Avezum A, Goodman SG, Flather MD. Predictors of hospital mortality in the global registry of acute coronary events. *Arch Intern Med.* 2003;163:2345.
- Antman EM, Cohen M, Bernink PJ, McCabe CH, Horacek T, Papuchis G, Mautner B, Corbalan R, Radley D, Braunwald E. The TIMI risk score for unstable angina/non-ST elevation MI: a method for prognostication and therapeutic decision making. *JAMA.* 2000;284:835–842.
- Goldberger JJ, Subacius H, Patel T, Cunnane R, Kadish AH. Sudden cardiac death risk stratification in patients with nonischemic dilated cardiomyopathy. *J Am Coll Cardiol.* 2014;63:1879–1889.
- Syed Z, Stultz CM, Scirica BM, Guttag JV. Computationally generated cardiac biomarkers for risk stratification after acute coronary syndrome. *Sci Transl Med.* 2011;3:102ra195.
- Bauer A, Kantelhardt JW, Barthel P, Schneider R, Mäkkitalo T, Ulm K, Hnatkova K, Schöming A, Huikuri H, Bunde A, Malik M, Schmidt G. Deceleration capacity of heart rate as a predictor of mortality after myocardial infarction: cohort study. *Lancet.* 2006;367:1674–1681.
- Barthel P, Schneider R, Bauer A, Ulm K, Schmitt C, Schomig A, Schmidt G. Risk stratification after acute myocardial infarction by heart rate turbulence. *Circulation.* 2003;108:1221–1226.
- Bauer A, Barthel P, Schneider R, Ulm K, Muller A, Joeing A, Stich R, Kiviniemi A, Hnatkova K, Huikuri H, Schomig A, Malik M, Schmidt G. Improved stratification of autonomic regulation for risk prediction in post-infarction patients with preserved left ventricular function (ISAR-Risk). *Eur Heart J.* 2009;30:576–583.
- Heart rate variability. Standards of measurement, physiological interpretation, and clinical use. Task Force of the European Society of Cardiology and the North American Society of Pacing and Electrophysiology. *Eur Heart J.* 1996;17:354–381.
- Kleiger RE, Stein PK, Bigger JT. Heart rate variability: measurement and clinical utility. *Ann Noninvasive Electrocardiol.* 2005;10:88–101.
- Schmidt G, Malik M, Barthel P, Schneider R, Ulm K, Rolnitzky L, Camm AJ, Bigger JT Jr, Schöming A. Heart-rate turbulence after ventricular premature beats as a predictor of mortality after acute myocardial infarction. *Lancet.* 1999;353:1390–1396.
- Chia C-C, Syed Z. Computationally generated cardiac biomarkers: heart rate patterns to predict death following coronary attacks. *SDM.* ; 2011:735–746.
- Raeder EA, Rosenbaum DS, Bhasin R, Cohen RJ. Alternating morphology of the QRST complex preceding sudden death. *N Engl J Med.* 1992;326:271–272.
- Syed Z, Scirica BM, Mohanavelu S, Sung P, Michelson EL, Cannon CP, Stone PH, Stultz CM, Guttag JV. Relation of death within 90 days of non-ST-elevation acute coronary syndromes to variability in electrocardiographic morphology. *Am J Cardiol.* 2009;103:307–311.
- Syed Z, Guttag JV. Identifying patients at risk of major adverse cardiovascular events using symbolic mismatch. *Adv Neural Inf Proc Syst.* 2010;23:2262–2270.
- de Lemos JA, Morrow DA, Bentley JH, Omland T, Sabatine MS, McCabe CH, Hall C, Cannon CP, Braunwald E. The prognostic value of B-type natriuretic peptide in patients with acute coronary syndromes. *N Engl J Med.* 2001;345:1014–1021.
- Cannon CP, Husted S, Harrington RA, Scirica BM, Emanuelsson H, Peters G, Storey RF; D-Investigators. Safety, tolerability, and initial efficacy of AZD6140, the first reversible oral adenosine diphosphate receptor antagonist, compared with clopidogrel, in patients with non-ST-segment elevation acute coronary syndrome: primary results of the DISPERSE-2 trial. *J Am Coll Cardiol.* 2007;50:1844–1851.
- Morrow DA, Scirica BM, Karwatowska-Prokopczuk E, Murphy SA, Budaj A, Varshavsky S, Wolff AA, Skene A, McCabe CH, Braunwald E. Effects of ranolazine on recurrent cardiovascular events in patients with non-ST-elevation acute coronary syndromes. *JAMA.* 2007;297:1775–1783.
- Morrow DA, Scirica BM, Karwatowska-Prokopczuk E, Skene A, McCabe CH, Braunwald E. Evaluation of a novel anti-ischemic agent in acute coronary syndromes: design and rationale for the metabolic efficiency with ranolazine for less ischemia in non-ST-elevation acute coronary syndromes (MERLIN-TIMI 36). *Am Heart J.* 2006;152:400. e401–400. e409
- Scirica BM, Morrow DA, Hod H, Murphy SA, Belardinelli L, Hedgepeth CM, Molhoek P, Verheugt FW, Gersh BJ, McCabe CH. Effect of ranolazine, an antianginal agent with novel electrophysiological properties, on the incidence of arrhythmias in patients with non-ST-segment-elevation acute coronary syndrome results from the Metabolic Efficiency With Ranolazine for Less Ischemia in Non-ST-Elevation Acute Coronary Syndrome—Thrombolysis in Myocardial Infarction 36 (MERLIN-TIMI 36) Randomized Controlled Trial. *Circulation.* 2007;116:1647–1652.
- Deboer RW, Karemker JM, Strackee J. Comparing spectra of a series of point events particularly for heart rate variability data. *IEEE Trans Biomed Eng.* 1984;31:384–387.
- Lisenby MJ, Richardson PC. The Beatquency Domain: an unusual application of the fast Fourier transform. *IEEE Trans Biomed Eng.* 1977;24:405–408.
- Laguna P, Ruiz M, Moody G, Mark R. Repolarization alternans detection using the KL transform and the Beatquency spectrum. *Comput Cardiol.* 1996;1996:673–676.
- Syed Z, Sung P, Scirica BM, Morrow DA, Stultz CM, Guttag JV. Spectral energy of ECG morphologic differences to predict death. *Cardiovasc Eng.* 2009;9:18–26.
- Goldberger AL, Amaral LA, Glass L, Hausdorff JM, Ivanov PC, Mark RG, Mietus JE, Moody GB, Peng C-K, Stanley HE. PhysioBank, PhysioToolkit, and PhysioNet components of a new research resource for complex physiologic signals. *Circulation.* 2000;101:e215–e220.
- Li Q, Mark RG, Clifford GD. Robust heart rate estimation from multiple asynchronous noisy sources using signal quality indices and a Kalman filter. *Physiol Meas.* 2008;29:15.
- De Chazal P, O'Dwyer M, Reilly RB. Automatic classification of heartbeats using ECG morphology and heartbeat interval features. *IEEE Trans Biomed Eng.* 2004;51:1196–1206.
- Zou KH, O'Malley AJ, Mauri L. Receiver-operating characteristic analysis for evaluating diagnostic tests and predictive models. *Circulation.* 2007;115:654–657.

28. Nearing BD, Verrier RL. Modified moving average analysis of t-wave alternans to predict ventricular fibrillation with high accuracy. *J Appl Physiol*. 2002;92:541–549.
29. Cox DR. Regression models and life-tables. *J Roy Stat Soc B*. 1972;187–220.
30. Cook NR. Statistical evaluation of prognostic versus diagnostic models: beyond the roc curve. *Clin Chem*. 2008;54:17–23.
31. Pencina MJ, D'Agostino RB, Steyerberg EW. Extensions of net reclassification improvement calculations to measure usefulness of new biomarkers. *Stat Med*. 2011;30:11–21.
32. La Rovere MT, Bigger JT Jr, Marcus Fl, Mortara A, Schwartz PJ. Baroreflex sensitivity and heart-rate variability in prediction of total cardiac mortality after myocardial infarction. ATRAMI (autonomic tone and reflexes after myocardial infarction) investigators. *Lancet*. 1998;351:478–484.
33. Buccelletti E, Gilardi E, Scaini E, Galiuto L, Persiani R, Biondi A, Basile F, Silveri NG. Heart rate variability and myocardial infarction: systematic literature review and metanalysis. *Eur Rev Med Pharmacol Sci*. 2009;13:299–307.
34. Stein PK, Barzilay JI, Chaves PH, Mistretta SO, Domitrovich PP, Gottdiener JS, Rich MW, Kleiger RE. Novel measures of heart rate variability predict cardiovascular mortality in older adults independent of traditional cardiovascular risk factors: the cardiovascular health study (CHS). *J Cardiovasc Electrophysiol*. 2008;19:1169–1174.
35. Verrier RL, Klingenheben T, Malik M, El-Sherif N, Exner DV, Hohnloser SH, Ikeda T, Martínez JP, Narayan SM, Nieminen T. Microvolt T-wave alternans physiological basis, methods of measurement, and clinical utility—consensus guideline by international society for Holter and Noninvasive Electrocardiology. *J Am Coll Cardiol*. 2011;58:1309–1324.
36. Yu H, Pi-Hua F, Yuan W, Xiao-Feng L, Jun L, Zhi L, Sen L, Zhang S. Prediction of sudden cardiac death in patients after acute myocardial infarction using T-wave alternans: a prospective study. *J Electrocardiol*. 2012;45:60–65.
37. Ben-Haim SA, Becker B, Edoute Y, Kochanovski M, Azaria O, Kaplinsky E, Palti Y. Beat-to-beat electrocardiographic morphology variation in healed myocardial infarction. *Am J Cardiol*. 1991;68:725–728.
38. Belie N, Gardin JM. ECG manifestations of myocardial ischemia. *Arch Intern Med*. 1980;140:1162.
39. Liu CK, Greenspan G, Piccirillo RT. Atrial infarction of the heart. *Circulation*. 1961;23:331–338.
40. Berger RD, Kasper EK, Baughman KL, Marban E, Calkins H, Tomaselli GF. Beat-to-beat qt interval variability novel evidence for repolarization lability in ischemic and nonischemic dilated cardiomyopathy. *Circulation*. 1997;96:1557–1565.